Biophysical Chemistry 135 (2008) 32–40

Contents lists available at ScienceDirect

Biophysical Chemistry

journal homepage: http://www.elsevier.com/locate/biophyschem

Influence of membrane potentials upon reversible protonation of acidic residues from the OmpF eyelet

Alina Asandei [1], Loredana Mereuta [1], Tudor Luchian *

'Al. I. Cuza' University, Faculty of Physics, Laboratory of Biophysics & Medical Physics, Blvd. King Carol I, No. 11, Iasi, R-700506, Romania

ARTICLE INFO

Article history:
Received 31 January 2008
Received in revised form 29 February 2008
Accepted 29 February 2008
Available online 10 March 2008

Keywords:
Single molecule recordings
Lipid membranes
OmpF
Spectral analysis
Membrane potentials
Protonation

ABSTRACT

In this research we employed single-molecule electric recording techniques to investigate effects of the transmembrane and dipole potential on the reversible protonation of acidic residues from the constriction zone of the OmpF porin. Our results support the paradigm according to which the protonation state of aspartate 113 and glutamate 117 residues from the constriction region of OmpF is influenced by the electric potential profile, via an augmentation of the local concentration of protons near these residues mediated by increasing negative transmembrane potentials. We propose that at constant bulk pH, pK_a values for proton bindings at these residues increase as the applied transmembrane potential increases in its negative values. Our data demonstrate that the apparent pK_a for proton binding of the acidic aminoacids from the constriction region of OmpF is ionic strength-dependent, in the sense that a low ionic strength in the aqueous phase promotes the increase of the protonation reaction rate of such residues, at any given holding potential. Supplementary, we present evidence suggesting that lower values of the membrane dipole potential lead to an increase in the values of the 'on' rate of the eyelet acidic residues protonation, caused by an elevation of the local concentration of hydrogen ions. Altogether, these results come to support the paradigm according to which transmembrane and dipole potentials are critical parameters for the titration behavior of protein sites embedded lipid membranes.

1. Introduction

One of the fundamental chemical reactions encountered in the biological world is the proton bindings reaction, which plays critical roles in protein structure and function. That is, reversible proton bindings are elementary steps for the transfer of protons within proteins, which stand as crucial in biochemical catalysis and energy transduction processes. A great deal of both theoretical and experimental approaches has been devoted over the decades to the accurate determination of aminoacid pK_as in proteins [1–6]. This was partly due to the fact that, for instance, pK_a's knowledge of the residues from the active site of an enzyme pinpoints the plausible proton donors and acceptors, and therefore helps in understanding the reaction mechanism [1,7,8]. Equally important, it is well-known that the stability of proteins and of several protein-ligand aggregates varies as a function of the ionization state of titratable aminoacid residues [9–12].

With paramount importance for the biological world, within folded proteins pK_a values of ionizable residues are usually shifted with respect to their aqueous solution values. With regard to this, a consensus over major determinants which promote pK_a's shifts has been reached, including here: contributions stemming from the Born solvation energy, the group's interaction with partial charges on the protein such as the peptide dipoles (so-called background charge interactions) and the group's interaction with other ionizable groups in the protein [2,13,14]. From a mathematical standpoint, estimations of pK_a's shifts in proteins are usually computed with the help of the linearized Poisson–Boltzmann equation. Notably, in an experimental attempt towards understanding the effect of the protein environment on the pK_a values of protein residues, protonatable side chains were engineered into the pore domain of the muscle nicotinic acetylcholine receptor, and large negative pK_a shifts for basic aminoacid residues in nonaqueous environments were reported [15].

In addition to the arguments presented above and taking into account that local electric fields in proteins alter the ion binding energy as compared to the bulk solution, it is very plausible that lipid membranes electric profile possesses the potential to influence via long-range interactions the equilibrium constant of hydrogen ions interaction with various residues, and implicitly the pK_a values. The most common electrical potentials associated with lipid membranes are the transmembrane potential difference, generated by a gradient of electric charge across the phospholipid bilayer and the membrane surface potential, which stems from the net excess electric superficial charges at the membrane interface in contact with the aqueous medium [16].

To date, electrostatic interactions are known to play extensive role in various aspects of protein structure and function, including here

* Corresponding author. Tel.: +40 232 201191; fax: +40 232201150.
E-mail address: luchian@uaic.ro (T. Luchian).
[1] These authors contributed equally to this work.

0301-4622/$ – see front matter © 2008 Elsevier B.V. All rights reserved.
doi:10.1016/j.bpc.2008.02.018

enzyme catalysis, ligand binding, the fine-tuning of redox potentials, and stability of folded proteins. At the microscopic level, the membrane potential was shown to alter the configurational equilibrium and the orientation of membrane-bound proteins [17–19]. On the other hand, the surface potential was proven to play important roles in cell adhesion and spreading, chemotaxis processes, binding of various anesthetics and ion channel antagonists [20–22]. In addition, a component of the electric membrane potential known as the dipole potential was acknowledged to play important roles in peptides–membrane interactions [23]. Its overall value (~300 mV, positive toward the membrane interior) and the correspondingly high electric field associated with it over the aqueous phase–hydrocarbon region interface (10^8–10^9 V m^{-1}), endow the dipole potential with major roles in the modulation of molecular processes which take place within a biomembrane, including protein insertion and functioning, kinetics and electrical conductance of certain aqueous protein pores [24–27].

In a recent contribution, within the framework of continuum electrostatics, authors employed a modified Poisson–Boltzmann equation to include the membrane potential component and presented evidence that the protonation probability of bacteriorhodopsin's aspartate 85 and aspartate 115 which take up protons from different sides of the membrane is differently influenced by the membrane potential [28].

In this work we employed single-molecule electric recording techniques on the OmpF porin inserted in artificial lipid membranes, to investigate effects of the transmembrane and dipole potential on the reversible protonation of acidic residues which are part of the constriction zone of the porin. The outer membrane porin F (OmpF) resembles a β-barrel structure, which possesses sixteen anti-parallel strands connected by turns at the periplasmic side and loops at the extracellular side of the bacteria they reside on [29]. One of the eight extracellular loops (L3) folds back into the pore lumen and about half way down the channel, an aspartate (D113) and glutamate (E117) from the tip of L3 face three arginine groups located at the channel wall (R42, R82 and R132), creating an asymmetrically shaped constriction zone of about 0.7 × 1.1 nm^2 in area. The transversal electric field on the constriction zone changes its modulus with changes in the solution acidity, fact that is intrinsically linked to the pH-dependent charged state of the residues making up that region [30,31]. As it has been nicely demonstrated, aqueous pH changes alter channel's conductance as a result of the direct interactions of fluctuating residue charges with penetrating ions, and the ensuing stepwise current transients observed mostly close to the pK_a values of the aminoacids located on the constriction zone reveal information about their reversible protonation mechanism [32]. There is plenty of evidence demonstrating that besides the OmpF porin, reversible protonation of ionizable residues induces conductance fluctuations in other ion conducting proteins, including here the α-hemolysin channel [33], Ca^{2+} [34] and mouse nicotinic AChR channels [15,35].

Our work suggests that both transmembrane potential and membrane dipole potential alter the kinetics of the reversible protonation of acidic residues with propensity to alter transport properties of the OmpF porin, with most plausible candidates in this respect being aspartate 113 and glutamate 117 residues, and implicitly modify the pK_as of such acidic aminoacid residues from the constriction site of the protein. We monitored the stepwise current flickering of the OmpF porin inserted in model lipid membranes at a pH value of 2.8, which ensured an optimal resolving accuracy in the power spectra changes of such fluctuations, once the protonation equilibrium of acidic residues, in particular the aspartate 113 and glutamate 117 residues would shift as a result of their electrostatic interactions with lipid bilayer potentials. By approximating power spectra of the current fluctuations with single Lorentzians, our data prove that more negative transmembrane potentials applied with respect to the OmpF addition side of the membrane, promote a faster reversible protonation of such residues. Assuming that such negative transmembrane potential values do little to the energy of the activated complex which characterizes the chemistry of reversible protonation of aspartate 113 and glutamate 117 residues, which plausibly are the preferred candidates to explaining the stepwise current transients through the OmpF porin observed in the acidic range, our results point to an augmentation in the local concentration of protons near these residues, caused by the electric interaction between positively charged protons and the electric potential within the membrane core. As a result of this, it is conceivable that at constant bulk pH, pK_a values for proton bindings at these residues would increase as the applied transmembrane potential increases in its negative values. In addition, we show that the observed phenomenon is ionic strength-dependent; as the Debye–Hückel theory predicts.

We also prove that when added from the cis side of the membrane, phloretin, a known compound for its ability to lower the membrane dipole potential, induces a similar change in the protonation equilibrium of the aspartate 113 and glutamate 117 residues, at any given holding transmembrane potential. This phenomenon comes in good physical agreement with the previously studied herein, since by either modifying the transmembrane holding potential towards negative values or by keeping its value constant but lowering the dipole potential of the membrane, one arrives at circumstances whereby the algebraic value of the electric potential at a point halfway across the hydrophobic core of the membrane decreases.

One very interesting feature of the OmpF porin lies in its change in selectivity with aqueous acidity [30]. In the end, we tested whether charge distribution alterations within the permeation pathway of the OmpF protein, as they are induced by dipole potential alterations and visible in our experiments for acidic aminoacids from the constriction region, lead to any visible changes on its selectivity. Thus far, current–voltage diagrams drawn for the OmpF porin in the absence and presence of phloretin under asymmetrical salt concentration point to no convincing evidence in support of this speculation.

2. Materials and methods

Electrophysiology experiments were carried out in the folded bilayer membranes system obtained with Montal–Mueller technique, as previously described [25,36]. The lipid used was L-α-phosphatidylcholine (Fluka, code 61755), and sodium chloride salt solutions were buffered at a pH value of 2.8 in 5 mM MES buffer (Sigma-Aldrich). Single channel insertion of the OmpF protein was achieved by adding ~1 μl from a dilute stock solution made in 1 M NaCl and 1% (v/v) of octyl POE to the cis chamber only, connected to the ground. Spontaneous channel insertion was usually obtained within a few minutes under stirring. The purified OmpF protein was a precious gift from Prof. Mathias Winterhalter (Bremen, Germany). When employed, phloretin (Fluka) was added to the cis side of the membrane, from a 0.1 M stock solution made in ethanol. Currents from the bilayer chamber were detected and amplified with a resistive headstage patch-clamp amplifier (EPC 8, HEKA, Germany) set to the voltage-clamp mode, via a pair of Ag/AgCl electrodes. Amplified electric signals were low-pass filtered at 10 kHz with the help of an active low-pass filter (LPF-8, Warner Instrument Corp., USA), and data acquisition was performed with a NI PCI 6014, 16-bit acquisition board (National Instruments, USA) at a sampling frequency of 30 kHz within the LabVIEW 8.20 environment. Numerical analysis, including time-domain low-pass filtering, spectral analysis and graphing, were done with the help of the Origin 6 software (OriginLab, USA). Fast Fourier analysis was performed on 2048 Hamming windowed data points, and at least 50 data segments were used to produce an averaged output. All experiments were performed at a room temperature of ~23 °C. When ion selectivity of the OmpF channel was studied, we used a salt gradient of 0.1 M (cis side) KCl // 3 M (trans side) KCl (Sigma-Aldrich), buffered at a pH of 2.87 in 5 mM MES (Sigma-

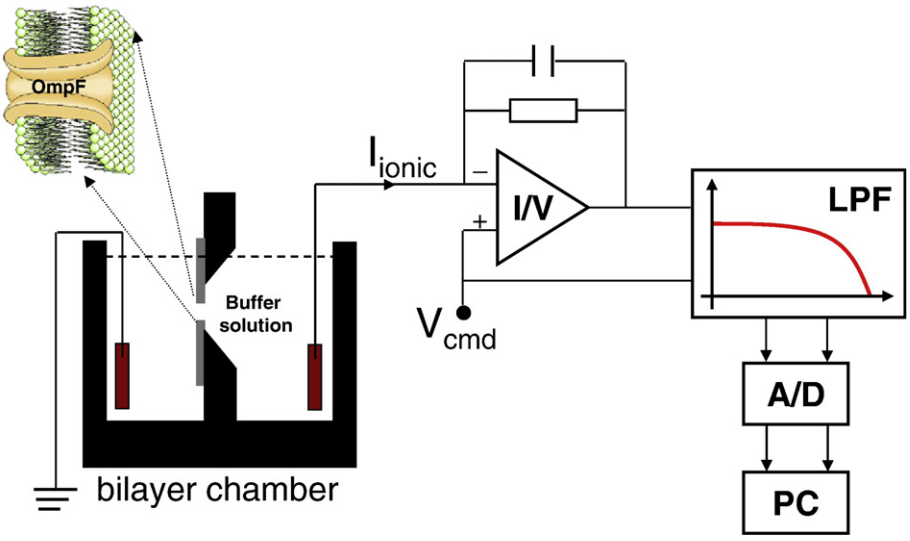

Fig. 1. The block diagram of the experimental setup used in our experiments: 'I/V' stands for the amplifier used to capture and amplify the ionic currents from the bilayer chamber , 'LPF' stands for hardware-based low-pass filter employed, 'A/D' represents the digitizer used for the analog-to-digital conversion of electric signals from the bilayer later fed into the computer ('PC').

Aldrich). During such experiments, Ag–AgCl electrodes were connected to the bilayer chamber via salt bridges made of agarose (~1% w/v) dissolved in 3 M KCl. Once the insertion of a single OmpF channel was achieved, a custom-designed virtual instrument written within the LabVIEW 2.0 environment was employed to automatically draw the current–voltage (I–V) diagrams. The charge selectivity of the OmpF channel ($\frac{P_{K^+}}{P_{Cl^-}}$) was assessed by measuring zero current potential (Ψ_{rev}), and by using an alternative form of the Goldman–Hodgkin–Katz equation:

$$\frac{P_{K^+}}{P_{Cl^-}} = \frac{[Cl^-]_{trans} - [Cl^-]_{cis}\exp(\frac{\Psi_{rev}F}{RT})}{[K^+]_{trans}\exp(\frac{\Psi_{rev}F}{RT}) - [K^+]_{cis}} \quad (1)$$

In expression (1), $[K^+]_{cis}$ and $[Cl^-]_{cis}$ refer to the concentration of potassium and chloride ions on the grounded (cis) side of the membrane, $[K^+]_{trans}$ and $[Cl^-]_{trans}$ the concentration of potassium and chloride ions on the opposite (trans) side, Ψ_{rev} is the measured reversal potential expresses in volt, and F, R, T have their usual thermodynamic meanings.

3. Results and discussion

One primary objective of this work was to quantify the influence exerted by the transmembrane potential upon conductance fluctuations of the OmpF porin, which are thought to stem mainly from the reversible protonation of ionizable sites from the constriction eyelet. To better succeed in this task, we monitored the stepwise current flickerings of the OmpF porin at a pH value close to 2.8, which should ensure an optimal resolving accuracy in voltage-induced power spectra changes of these fluctuations.

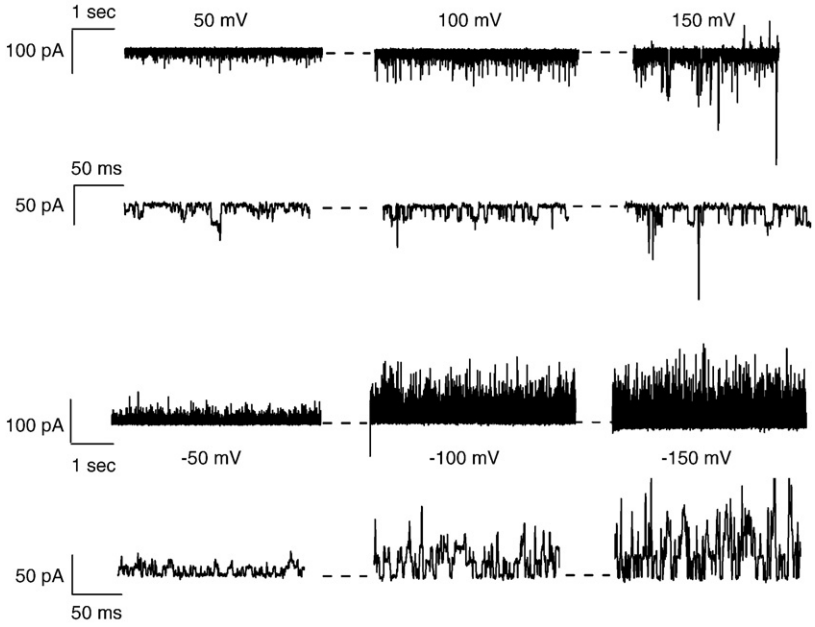

Fig. 2. Single-channel traces showing current fluctuations through a fully open OmpF channel at various holding potentials, at a pH value of 2.8. Downwards (at positive holding potentials) and upwards (at negative holding potentials) current flickerings relative to the fully open channel current baseline (dotted lines) reflect the reversible protonation of the aspartate 113 and glutamate 117 residues from the channel's constriction eyelet.

The block diagram of the setup used in our experiments is presented in Fig. 1.

As it has been previously described, such conductance fluctuations occur more frequently in acidic solutions, and in 1 M KCl there is a well defined peak around pH 2.5 (32); approximately two pH-units changes in either direction around this peak would lead to a very steep modification to the 'zero-frequency spectral density' of these fluctuations. We therefore reasoned that the effect of transmembrane potential upon current fluctuations of the OmpF porin would be better seen by setting the pH of the buffer solution where the slope reaches a maximal value, somewhere in the middle of the titration curve which characterizes the protonation equilibrium of the aspartate 113 and glutamate 117 residues, that is pH ~2.8.

In Fig. 2 we show representative original traces of current fluctuations through a fully open OmpF trimer recorded at various holding potentials, which are believed to reflect mostly the reversible protonation of the aspartate 113 and glutamate 117 residues from the channel's constriction eyelet. The multi-level appearance of the conductive behavior seen in these traces may be assigned to the fact that each of the monomers making up the OmpF trimer possesses at least two distinct side chains of ionizable aminoacids whose protonation–deprotonation activity leads to the 'single-monomer' current to fluctuate between at least two states, as a result of the net charge variation at the constriction eyelet. It is of interest to correctly assign the various sub-conductance states to the charged state of aspartate 113 and glutamate 117 residues, knowing that under relatively high acidic conditions, i.e. pH<4, the OmpF channel becomes anion-selective.

A tempting assertion in this respect would be that, whenever an extra electric charge appears within any of the OmpF monomers as a result of a deprotonation event involving either the aspartate 113 or the glutamate 117 residue, the net charge within the permeation pathway might hinder the anions electrodifussion, so that a step reduction of the resulting current ensues. Therefore, at positive potentials for instance, transiently downwards current reductions would be associated to the deprotonated states of the acidic residues from the constriction eyelet. It is noticeable from Fig. 2 that the noisiness of current fluctuations mediated by such reversible protonation events as described above vary strongly with the absolute value and the sign of the holding potential; as a crude example, the standard deviation of current fluctuation was evaluated at ~5 pA at +50 mV, ~18 pA at +150 mV, ~8 pA at −50 mV and ~26 pA at −150 mV. This in turn hints to a possible involvement of the transmembrane potential in the reversible protonation kinetics described herein.

Amplitude histograms depicted in Fig. 3 support the hypothesis according to which each of the two acidic residues from the constriction eyelet of any of the three monomers forming an OmpF oligomer behaves similarly from the point of view of current changes brought about by the reversible protonation it undergoes. That is, one can notice that the current through a fully open OmpF channel changes in almost similar steps whose value are dictated by the membrane holding potential only, although those current changes may originate from any of the aspartate 113 and glutamate 117 residues found on the three identical monomers of the protein.

In order to understand the extent to which the reversible protonation of the aspartate 113 and glutamate 117 residues is a voltage-dependent process, we next estimated power spectral densities of current fluctuations through a single, fully open OmpF channel, at different holding potentials. In Fig. 4 we show selected traces displaying the spectral characteristics of open channel current fluctuations measured at pH=2.8 at various holding potentials, and to facilitate the interpretation of effects caused by the transmembrane potential upon the protonation–deprotonation kinetics, all power spectral density traces were normalized.

Without digging into technical details which were described previously in an excellent manner [33,35,37], we restrict ourselves

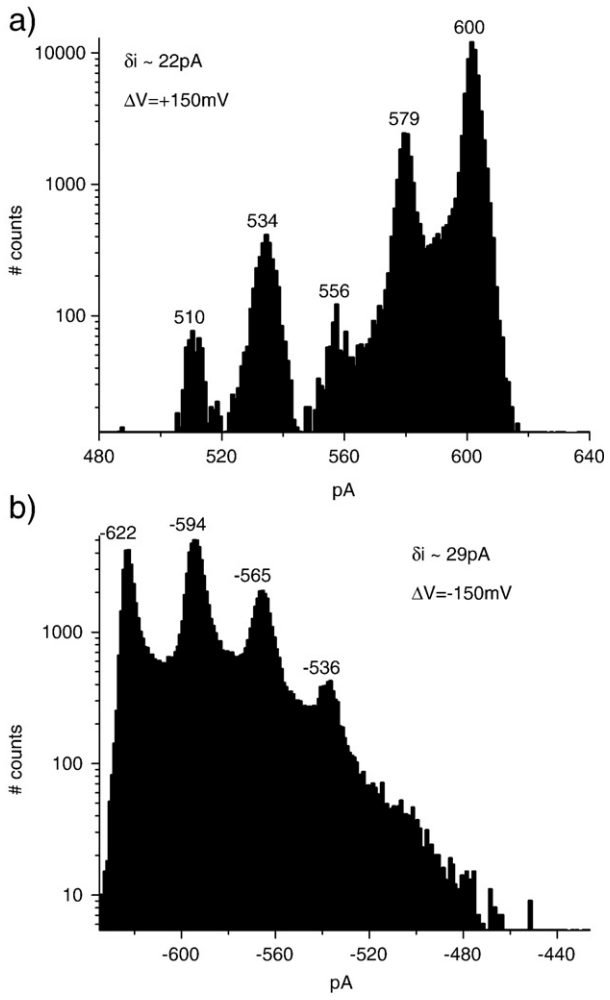

Fig. 3. Representative amplitude histograms of current fluctuations through a fully open OmpF channel measured at +150 mV (panel a) and −150 mV (panel b), caused by the reversible protonation of the aspartate 113 and glutamate 117 residues. The numeric values above each of the amplitude peaks denote step-amplitudes changes of electric current (in pA), stemming from the reversible protonation of the aspartate 113 or glutamate 117 residues from the protein trimer. Since at a given holding potential current changes occur in almost similar increments (δi ~22 pA at +150 mV and δi ~29 pA at −150 mV), we believe that each of the aspartate 113 and glutamate 117 residues from any of the three monomers of the OmpF channel behaves similarly from the point of view of electric changes imposed by the reversible protonation it undergoes upon ion transport through the channel.

only to stating that if one perceives protonation–deprotonation events of a given acidic aminoacid (R) from the OmpF eyelet as fluctuations of the open-channel current between two levels of different conductance, modeled in the frame two-state Markov processes:

$$R^- + H^+ \underset{k_{off}}{\overset{k_{on}}{\Leftrightarrow}} RH \tag{2}$$

the power density spectrum $S(f)$ of current fluctuations through the whole trimer is given by a 'Lorentzian' function:

$$S(f) = \frac{S(0)}{1 + \left(\frac{f}{f_c}\right)^2} \tag{3}$$

where:

- R^- and RH stand for the deprotonated and protonated state of any of the acidic aminoacids from the OmpF's eyelet, on any of the three monomers;
- k_{on} and k_{off} are the protonation and respectively deprotonation reaction constants;

- $S(0)$ is the constant value of the power density spectrum at small frequencies;
- $S(0)=4\cdot6\cdot(\delta i)^2\cdot p_{RH}\cdot(1-p_{RH})\cdot\tau$. The constant '6' appears in this expression as a result of the six possible sites where reversible protonation reactions occur (i.e., most likely aminoacids aspartate 113 and glutamate 117 from the three identical monomers of the protein), viewed as being similar and independent from the point of view of their kinetic behavior;
- relaxation time $\tau=\frac{1}{2\cdot\pi\cdot f_c}=\frac{1}{k_{on}\cdot[H^+]+k_{off}}$;
- P_{RH} is the stationary probability of the protonated state of the aminoacid;
- δi represents the current alteration through the open channel as a result of local electrostatic changes due to one aminoacid deprotonation. In the view of results embodied by Fig. 3, each of the aminoacids aspartate 113 and glutamate 117 from the three identical monomers of the protein behave similarly from the viewpoint of current alteration through the open channel, when undergoing the reversible protonation process;

It is visible from Fig. 4 that negative holding potentials favor an increase of the corner frequency (f_c). By assuming that the chemistry of the reversible protonations taking place at the acidic residues from the OmpF eyelet remains largely un-affected by the holding potential, i.e. intrinsic k_{on} and k_{off} reaction constants are not dependent on the holding potential, it becomes very plausible that elevated values of the corner frequency (f_c) at more negative holding potentials reflect an increase in the local concentration of hydrogen ions under such conditions, which leads to elevated values of the 'on' rate of the residues protonation.

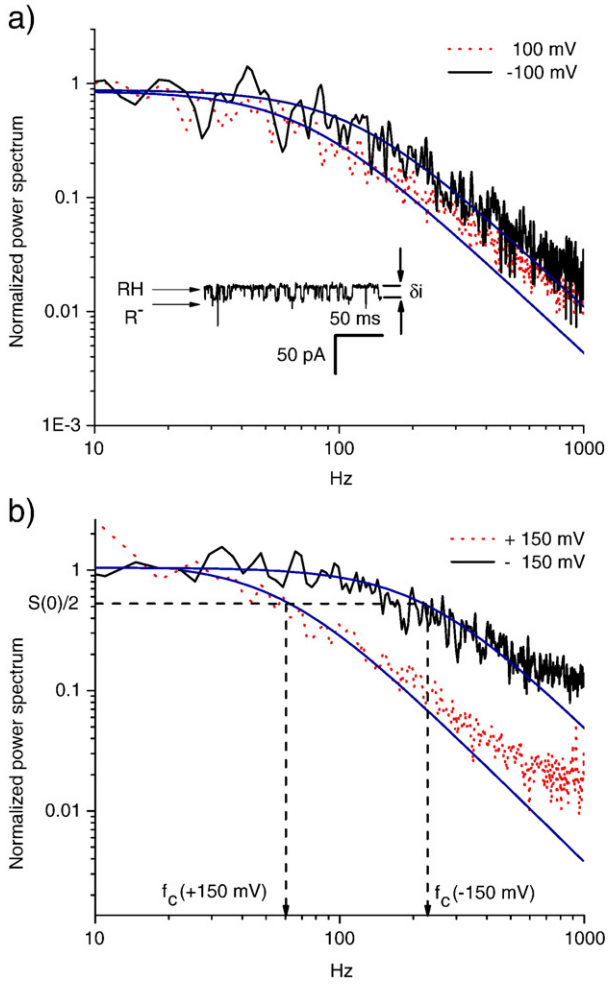

Fig. 4. Normalized power spectral densities of current fluctuations through a single, fully open OmpF channel in 2 M NaCl, at +100 mV; −100 mV (panel a) and +150 mV; −150 mV holding potentials (panel b). The inset in panel a shows, at a finer time scale, downward current transients stemming from the collective reversible protonation of acidic residues from the constriction zone of the OmpF trimer measured at +100 mV. Solid lines represent the best fit of power spectra made with a single Lorenzian. For the sake of comparison, we display in panel b the shift in the corner frequency (f_c) – which is a measure of the characteristic relaxation time of the reversible protonation processes – when the holding potential goes from +150 mV to −150 mV.

Taking into account the net negative charges at protonable carboxyl sidechain of acidic residues from the OmpF eyelet, this will result in substantial ionic strength-dependent point charge potentials, so that it is expected that the on-rate for hydrogen ion bindings will be elevated at low ionic strengths.

Based on the Debye–Hückel theory, one may state that the electric potential at the radial distance (r) around a point charge (ze^-) placed in an aqueous solution of relative electric permittivity (ε_r) containing various dissolved salts of valence (z_i) and bulk concentration (n_i) is given by:

$$\Psi(r)=\frac{z\cdot e^-}{4\cdot\pi\cdot\varepsilon_0\cdot\varepsilon_r}\frac{e^{-K\cdot r}}{r} \tag{4}$$

where:

- $K^2=\frac{2\cdot I\cdot(e^-)^2}{\varepsilon_0\cdot\varepsilon_r\cdot k\cdot T}$ (κ^{-1} is called the Debye screening length)
- $I=\frac{1}{2}\sum_i z_i^2\cdot n_i^{bulk}$ (ionic strength)
- n_i^{bulk} is the bulk value concentration of the 'i' ion species of valence 'z_i'
- e^- is the elementary electric charge, and ε_0 refers to vacuum's electric permittivity

Therefore, within the Poisson–Boltzmann formalism and at thermal equilibrium, one can write for the local concentration of hydrogen ions $[H^+](r)$ around a negatively charged carboxyl group:

$$[H^+](r)=[H^+]_{bulk}\cdot e^{-\frac{\Psi(r)}{k\cdot T}} \tag{5}$$

where:

- $[H^+]_{bulk}$ represents the bulk concentration of hydrogen ions, away from the electrostatic influence of the carboxyl group, modeled as a point charge and which generates the electric potential $\Psi(r)$.

From formula (5) it becomes clear that as the ionic strength of the aqueous solution decreases, so does the 'shielding' effect of ionic atmosphere on the electric potential of a negatively carboxyl group, and the local concentration of hydrogen ions will assume elevated values. The end result of this will be an increase on the protonation on-rate of acidic residues from the OmpF eyelet.

In direct relation to this, representative power spectral densities of current fluctuations measured through a single open OmpF channel at −100 mV and different salt concentrations (i.e., 0.5 M and 2 M NaCl) are being shown in Fig. 5, panel a. It is visible from such traces that at 0.5 M NaCl, the frequency corner of current fluctuations power spectrum increases with ~33% as compared to the 2 M NaCl case. By assuming a lack of ionic strength dependence of the intrinsic k_{on} and k_{off} reaction constants ($k_{on}^{0.5M}=k_{on}^{2M}=k_{on}$ and $k_{off}^{0.5M}=k_{off}^{2M}=k_{off}$), this phenomenon illustrates the augmenting effect mediated by point-charge electrostatic influence of negatively charged carboxyl group of acidic residues from the OmpF eyelet upon the local concentration of hydrogen ions. If we make once again use of the assumptions made above, it is clear that the algebraic difference between corner frequencies measured at 0.5 M to 2 M NaCl writes:

$$\begin{aligned} f_c(0.5M)-f_c(2M)&=\frac{k_{on}^{0.5M}[H^+]_{0.5M}+k_{off}^{0.5M}}{2\pi}-\frac{k_{on}^{2M}[H^+]_{2M}+k_{off}^{2M}}{2\pi}\\ &=\frac{k_{on}[\delta H^+]}{2\pi}=\text{const.}[\delta H^+] \end{aligned} \tag{6}$$

In this expression (6), by $[\delta H^+]$ we denote the upwards change of the local concentration of hydrogen ions brought about by the change of ionic strength of the aqueous solution from 2 M to 0.5 M NaCl, while the remaining factor $\left(\frac{k_{on}}{2\pi}\right)$ can be perceived as a constant, salt- and voltage-independent (const.). Interestingly, our results demonstrate that $[\delta H^+]$ gets considerably higher at more negative holding potentials (Fig. 5, panel b), and this again reflects the influence played by the transmembrane electric potential profile upon the local concentration of hydrogen ions within the OmpF pore.

In line with these experimental facts, it came natural for us to propose that by lowering the dipole potential on both sides of the membrane, a similar effect would occur with respect to changes of local proton concentrations near acidic residues from the constriction zone of the protein. In Fig. 6 we graphically layout our rationale in better details: so far, we have established that negative holding potentials across the membrane facilitate a higher proton concentration near the OmpF eyelet, located somewhere close to mid-plane of the membrane. That is to say, the higher is the negative holding potential in absolute value, the lesser is the electrostatic repelling influence sensed by protons within the OmpF pore when they interact

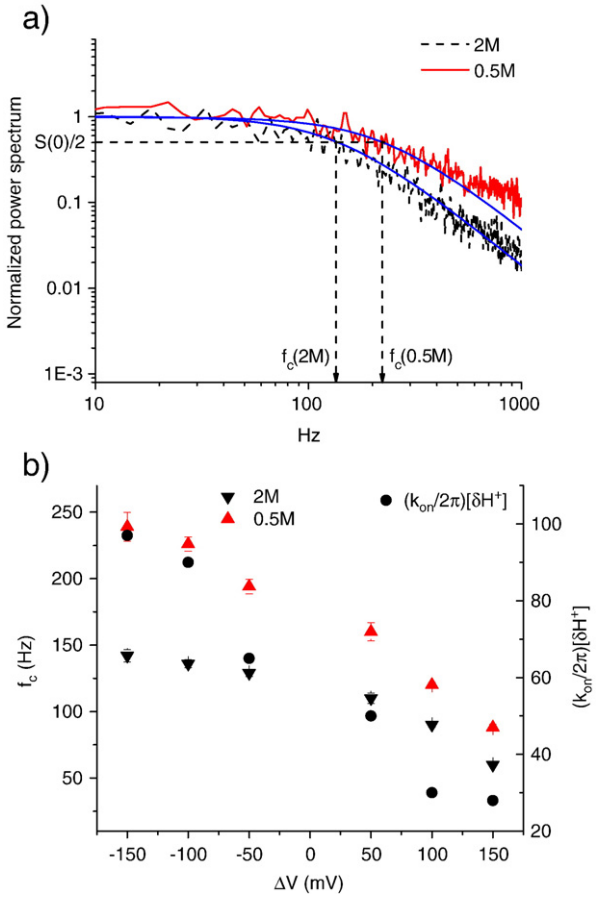

Fig. 5. (a) Normalized power spectra of current fluctuations measured through the OmpF trimer at −100 mV, showing the influence of ionic strength upon the corner frequency of reversible protonation-induced noise through the channel. At 0.5 M NaCl (solid line), the frequency corner of the power spectrum increases with ~33% as compared to the 2 M NaCl case (dashed line), which reflects the low salt-mediated increase in the local concentration of hydrogen ions around acidic residues from the constriction zone of the porin. (b) Voltage-dependence of corner frequencies of the reversible protonation-induced electric noise through the OmpF porin, at 0.5 M NaCl (upright triangles) and 2 M NaCl (inverted triangles). The change of the local concentration of hydrogen ions $[\delta H^+]$ caused by the change of ionic strength from 0.5 M to 2 M NaCl, does depend upon the holding potential, and this is reflected by the voltage dependence of the algebraic difference of corner frequencies measured at 0.5 M to 2 M NaCl (solid circles; see text). Data are represented as average values and standard deviations of the mean, as inferred from at least three experiments.

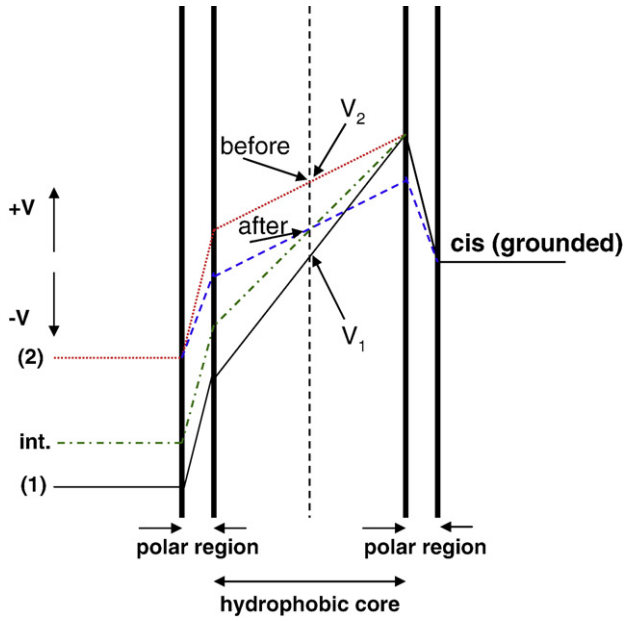

Fig. 6. Over-simplified depiction of the electric potential profile across a model lipid membrane, showing the increase of local potential values close to the mid-section of the membrane at more negative holding potentials (V1; solid line) compared to less negative ones (V2; dotted line). Starting from this case (applied potential difference denoted by the profile (2)), if the membrane dipole potential assumes a lower value on both sides of the membrane, the net result will be a lower value of the local potential anywhere within the membrane as compared to the control case (see the dashed electric profile, denoted by 'after'). From the perspective of local values changes of the electric potential within the membrane (compare V_{after} and V_{before}), by lowering the value of the dipole potential is similar to holding the membrane at a somewhat lower value of the potential difference; see the dashed-dotted electric profile, corresponding to an intermediary 'int.' holding potential ($V_{(2)} > V_{(int)} > V_{(1)}$).

with the membrane potential profile across the membrane. Compare for instance the value of the local potential values close to the mid-section of the membrane ($V_1 < V_2$) when the holding potential is set to various negative holding potentials whose membrane profiles are being depicted by (1) and (2), and $V_{holding}$ (1) < $V_{holding}$ (2).

As it is supported by the experimental evidence presented so far, an increase in the local concentration of hydrogen ions within the protein pore at the $V_{holding}$ (1) would reflect in an elevated value of the corner frequency (f_c) of the power density spectrum $S(f)$ which characterize kinetically current fluctuations induced in the open pore current by reversible protonations of acidic residues from the constriction zone. However, if at a given holding transmembrane potential the membrane dipole potential assumes a lower value, the net result will again be a lower value local potential value anywhere within the membrane as compared to the initial case ($V_{after} < V_{before}$).

To sum this up and from the view-point of changes in the local value of the electric potential within the membrane, by lowering the value of the dipole potential stands equivalent to imposing a lower value of the transmembrane holding potential, as depicted by the 'int.' potential profile.

Among others, phloretin has been often used as a molecular compound that reduces the lipid bilayers or monolayers positive dipole potential when adsorbed to the membrane, and its effect has been studied in details elsewhere [38,39]. Keeping in mind that only the neutral form of phloretin gets adsorbed to membrane bilayers or lipid monolayers, the induced decrease of the dipole potential will be enhanced as the pH of the aqueous solutions drops below its pK_a value (pH < 7.3). However, as the pH used throughout our experiments was ~2.8, we were aware of a relative loss in phloretin efficacy to decrease the membrane dipole potential, since it has been reported that below pH = 6 a declining tendency of phloretin-induced dipole potential changes sets in [40]. To try and compensate for this low pH-mediated loss of affinity, we choose to work at relatively high concentrations of phloretin (≥200 μM), well beyond the value where the

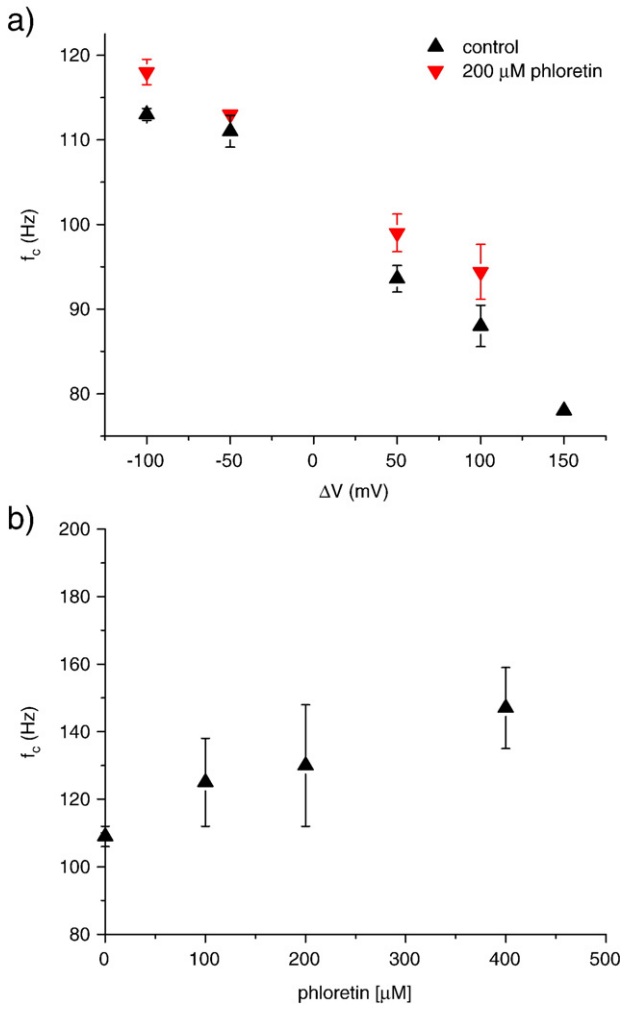

Fig. 7. (a) The effect of lowering the membrane dipole potential as induced by the cis application of 200 μM phloretin, upon the corner frequency of reversible protonation-induced noise through the OmpF channel. Elevated values of the corner frequency (f_c) measured at various holding potentials in the presence of phloretin, reflect an increase in the values of the 'on' rate of the eyelet acidic residues protonation, most likely caused by an augmentation of local concentration of hydrogen ions. (b) Higher values of the concentration of bulk phloretin result in increasingly lower local potential values within the membrane, which in turn augment the protonation kinetics of acidic residues from the protein eyelet via an increase of local protons concentration near the OmpF eyelet. In both panels data are represented as average values and standard deviations of the mean, as inferred from at least three experiments.

saturation effect of its dipole potentials-induced changes at mildly acidic values occurs (i.e., ~60 μM).

Our experiments with phloretin added on the cis side of the membrane do prove this predicted behavior of reversible protonation kinetics which accompany lowering the membrane dipole potential. In the presence of 200 μM phloretin, elevated values of the corner frequency (f_c) measured at various holding potentials reflect an increase in the values of the 'on' rate of the eyelet acidic residues protonation, most likely caused by an augmentation of local concentration of hydrogen ions. Interestingly, this effect is positively correlated to the phloretin concentration (Fig. 7, panel b); the higher the concentration of bulk phloretin, the higher will be its membrane-adsorbed concentration value leading to correspondingly lower local potential values within the membrane, via changes it imposes on the membrane dipole potential values. Due to the relatively high diffusion coefficient of phloretin across lipid bilayers (5.5×10^{-2} cm^2 s^{-1}, see Refs [40, 41]), it is not far fetched to assume that during the course of our experiments – which spanned 10 min or greater, phloretin equilibrates its gradient on both sides of the membrane, despite the fact that we added it initially to the cis side of the membrane only. Consequently, one may safely regard effects of phloretin upon the studied protonation kinetics as a consequence of dipole moment changes on both leaflets of the artificial membrane.

It is known from literature that the effective charge of the ionizable residues located near the lumen of the OmpF channel vary as a function of pH, and the associated electric field ensues a complex profile of potential within the ions pathway [30]. Moreover, plenty of previous data, points to the fact that cation/anion selectivity is accomplished via long-range electrostatic interactions, which are rather sensitive to the concentration of protons [42–44].

Based upon electrodiffusion considerations made within the Poisson–Boltzmann formalism, it may be predicted that the degree of protonation is expected to affect the cation/anion selectivity of the channel, and implicitly its reversal potential. We therefore asked whether charge distribution alterations within the permeation pathway of the OmpF protein, as they are induced by dipole potential alterations visible in our experiments for acidic aminoacids from the constriction region, lead to changes on its ion selectivity. Based the observed increase in the 'on' rate of protonation of aspartate 113 and glutamate 117 residues in the presence of phloretin, charge alterations are present to a certain extent within the permeation pathway of the OmpF channel, and caused by the shift in the ionization equilibrium established between the bulk protons and these residues.

The reversal potential of OmpF porin was determined by evaluating the null-current membrane potentials produced in the presence of salt gradients across the membrane. In Fig. 8 we show I–V diagrams which characterize transport properties of the OmpF porin in a (cis)0.1 M/(trans) 3 M KCl gradient at pH=2.87, in the absence (control) and presence of 200 μM phloretin added on the cis side of the membrane. From such data we inferred reversal potentials of 8.50±0.20 mV (average±S.E.M) under control conditions and 8.43±0.21 mV (average±S.E.M) with phloretin added in, and the calculated selectivity ratios of the OmpF porin showed no significant difference in the studied cases ($\frac{P_{K^+}}{P_{Cl^-}}$=0.704 control and $\frac{P_{K^+}}{P_{Cl^-}}$=0.706 in the presence of 200 μM phloretin). Therefore, open channel selectivity studies carried out at the single molecule level led us to conclude that dipole potential-induced changes of ionization equilibrium of acidic residues from the constriction site of the OmpF porin leave transport and selectivity properties of the protein largely unmodified.

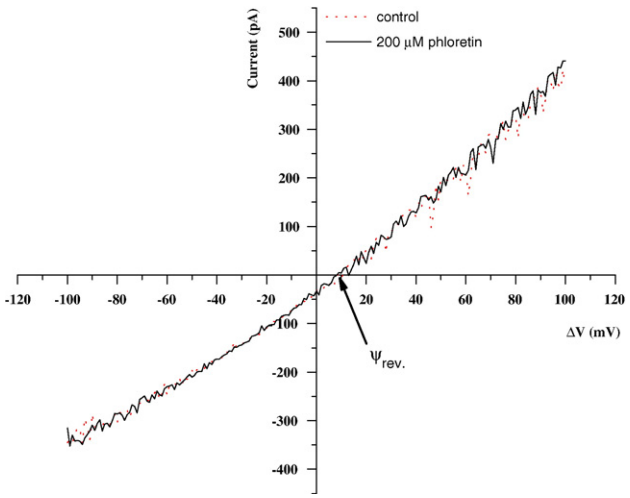

Fig. 8. Representative I–V diagrams which characterize transport properties of the OmpF porin in the absence (control) and presence of 200 μM phloretin added on the cis side of the membrane. Such experiments were carried out on the same protein, before and after addition of phloretin, in a (cis)0. 1M/(trans) 3M KCl gradient at pH=2.87. The practically un-changed values of the reversal potentials under such conditions i.e., 8.50±0.20 mV (average±S.E.M) under control conditions and 8.43±0.21 mV (average±S.E.M) with phloretin added, is an indicator of the fact that charge alterations induced within the permeation pathway of the OmpF channel by phloretin, leaves the cation/anion selectivity of the porin practically un-changed.

To this end, we must stress nevertheless that one crucial assumption made in interpretation of the data presented herein, is that current fluctuations seen at low pH values stem mostly from the reversible protonation of aspartate 113 and glutamate 117 residues. To further clarify and possibly support this assertion, we plan to carry out further experimental work with mutated OmpF proteins in which such residues will be replaced with non-titratable ones; provided that our assumption is correct all way through, a double mutation involving aspartate 113 and glutamate 117 residues should substantially reduce the low pH current fluctuations through the porin.

4. Concluding remarks

In this research we studied the electrostatic influence played by the transmembrane and dipole potential of artificial lipid membranes upon the ionization equilibrium of acidic aminoacids from the constriction site of the OmpF porin. For this, we have resorted to single-molecule electrophysiology experiments on the OmpF reconstituted in phosphatidylcholine lipid bilayers.

Results of noise spectral evaluations made on time-resolved current stepwise transients at pH 2.8 unveil that protonation of aspartate 113 and glutamate 117 residues from the OmpF's eyelet region performs vectorially, being favored at lower algebraic values of the local electric potential.

Our main findings are:

- Protonation states of aspartate 113 and glutamate 117 residues from the constriction region of OmpF are influenced by the electric potential profile, whereby more negative transmembrane potentials augment the local concentration of protons near these residues. Consequently, we propose that at constant bulk pH, pK_a values for protons binding at these residues increase as the applied transmembrane potential goes up in its negative values.
- The apparent pK_a for proton binding of the acidic aminoacids from the constriction region of OmpF is ionic strength-dependent; as the electrostatic potential around the negatively charged carboxyl groups which make up these centers becomes less screened-out by the ionic strength in the aqueous phase, the 'on' reaction rate for the protonation of such residues gets augmented at any given holding potential.
- Membrane dipole potential changes prove effective in altering the protonation equilibrium of the aspartate 113 and glutamate 117 residues at any given holding transmembrane potential, and lower values of it cause an increase in the values of the 'on' rate of the eyelet acidic residues protonation, most likely caused by an augmentation of local concentration of hydrogen ions.

These observations constitute direct proof in favor of electrostatic interactions between lipid membrane potential profiles and penetrating hydrogen ions through the OmpF porin, and shed new light on the paradigm according to which transmembrane and dipole potentials are critical parameters for the titration behavior protein sites embedded in a lipid membrane.

Future experiments involving mutagenesis approaches will bring new knowledge into the important issues of how protons accessibility to aminoacid reaction centers and changes in the electrostatic features in the immediate vicinity of such centers, as caused for instance by orientation of various side chains relative to the ion pathway [45,46] modulate the titration behavior of pore-exposed protein sites, and reveal roles played by the titration states of pore-lining aminoacids in OmpF in setting transport properties of the protein [47,48]. This we believe will help elucidate structural and functional aspects of open protein pores.

Acknowledgments

We greatly acknowledge the financial support offered by the Romanian Ministry of Research and Technology through grants CEEX 168/2006 (TL) and CEEX 239/2006 (TL). We would also like to express our deep thanks to Prof. Mathias Winterhalter (Bremen, Germany) for the purified OmpF protein.

References

[1] A. Warshel, Calculations of enzymic reactions: calculations of pK_a, proton transfer reactions, and general acid catalysis reactions in enzymes, Biochemistry 20 (1981) 3167–3177.
[2] D. Bashford, M. Karplus, pK_a's of ionizable groups in proteins: atomic detail from a continuum electrostatic model, Biochemistry 29 (1990) 10219–10225.
[3] D. Bashford, K. Gerwert, Electrostatic calculations of the pK, values of ionizable groups in bacteriorhodopsin, J. Mol. Biol. 224 (1992) 473–486.
[4] T. Simonson, J. Carlsson, D. Case, Proton binding to proteins: pK_a calculations with explicit and implicit solvent models, J. Am. Chem. Soc. 126 (1993) 4167–4180.
[5] G. Del Buono, F. Figueirido, R. Levy, Intrinsic pK_a's of ionizable residues in proteins: an explicit solvent calculation for lysozyme, Proteins 20 (1994) 85–97.
[6] Y.Y. Sham, Z.T. Chu, A. Warshel, Consistent calculations of pK_a's of ionizable residues in proteins: Semi-microscopic and microscopic approaches, J. Phys. Chem. B. 101 (1997) 4458–4472.
[7] X. Raquet, V. Lounnas, J. Lamotte-Brasseur, J. Frere, R. Wade, pK_a calculations for class a -lactamases: methodological and mechanistic implications, Biophys. J. 73 (1997) 2416–2426.
[8] J.E. Nielsen, J.A. McCammon, Calculating pK_a values in enzyme active sites, Protein Science 12 (2003) 1894–1901.
[9] A. Yang, B. Honig, On the pH dependence of protein stability, J. Mol.Biol. 231 (1993) 459–474.
[10] M. Schaefer, M. Karplus, pH-dependence of protein stability: absolute electrostatic free energy differences between conformations, J. Phys. Chem. B. 101 (1997) 1663–1683.
[11] D. Morikis, A.H. Elcock, P.A. Jennings, J.A. McCammon, Native state conformational dynamics of GART: a regulatory pH-dependent coil-helix transition examined by electrostatic calculations, Protein Science 10 (2001) 2363–2378.
[12] A.M. Mackerell, M.S. Sommer, M. Karplus, pH dependence of binding reactions from free energy simulations and macroscopic continuum electrostatic calculations: application to 2'GMP/3'GMP binding to Ribonuclease T1 and implications for catalysis, J. Mol. Biol. 247 (1995) 774–807.
[13] J. Antosiewicz, J.A. McCammon, M.K. Gilson, Prediction of pH-dependent properties of proteins, J. Mol. Biol. 238 (1994) 415–436.
[14] G. Archontis, T. Simonson, Proton binding to proteins: a free energy component analysis using a dielectric continuum model, Biophys J 88 (2005) 3888–3904.
[15] G.D. Cymes, Y. Ni, C. Grosman, Probing the structure and electrostatics of ion-channel pores one proton at a time, Nature 438 (2005) 975–980.
[16] P. O'Shea, Physical landscapes in biological membranes: physico-chemical terrains for spatio-temporal control of biomolecular interactions and behaviour, Phil. Trans. R. Soc. A 363 (2005) 575–588.
[17] C. Kempf, R.D. Klausner, J.N. Weinstein, J. Van Renswoude, M. Pincus, R. Blumenthal, Voltage-dependent trans-bilayer orientation of melittin, J. Biol. Chem. 257 (1982) 2469–2476.
[18] B. Roux, Influence of the membrane potential on the free energy of an intrinsic protein, Biophys. J. 73 (1997) 2980–2989.
[19] D.S. Cafiso, Alamethicin: a peptide model for voltage gating and protein-membrane interactions, Annu. Rev. Biophys. Biomol. Struct. 23 (1994) 141–165.
[20] S. McLaughlin, A. Aderem, The myristoyl-electrostatic switch: a modulator of reversible protein–membrane interactions, TIBS. 20 (1995) 272–276.
[21] J.J. Volwerk, P.C. Jost, G.H. de Haas, O.H. Griffith, Activation of porcine pancreatic phospholipase A2 by the presence of negative charges at the lipid-water interface, Biochemistry 25 (1986) 1726–1733.
[22] L. Wojtczak, K.S. Famulski, M.J. Nalecz, J. Zborowski, Influence of the surface potential on the Michaelis constant of membrane-bound enzymes: effect of membrane solubilization, FEBS Lett. 139 (1982) 221–224.
[23] G. Cevc, Membrane electrostatics, Biochim. Biophys. Acta 1031 (1990) 311–382.
[24] S.H. White, A.S. Ladokhin, S. Jayasinghe, K. Hristova, How membranes shape protein structure, J. Biol. Chem. 276 (2001) 32395–32398.
[25] T. Luchian, L. Mereuta, Phlorizin-and 6-Ketocholestanol-mediated antagonistic modulation of alamethicin activity in phospholipid planar membranes, Langmuir 22 (2006) 8452–8457.
[26] B. Maggio, Modulation of phospholipase A2 by electrostatic fields and dipole potential of glycosphingolipids in monolayers, J. Lipid Res. 40 (1999) 930–939.
[27] J. Cladera, P. O'Shea, Intramembrane molecular dipoles affect the membrane insertion and folding of a model amphiphilic peptide, Biophys. J. 74 (1998) 2434–2442.
[28] E. Bombarda, T. Becker, G.M. Ullmann, Bacteriorhodopsin: insights from electrostatic calculations into the regulation of proton pumping, JACS 128 (37) (2006) 12129–12139.
[29] T. Schirmer, General and specific porins from bacterial outer membranes, J. Struct. Biol 121 (1998) 101–109.
[30] A. Alcaraz, E.M. Nestorovich, M. Aguilella-Arzo, V.M. Aguilella, S.M. Bezrukov, Salting out the ionic selectivity of a wide channel: the asymmetry of OmpF, Biophys. J. 87 (2004) 943–957.
[31] D.J. Muller, A. Engel, Voltage and pH-induced channel closure of porin OmpF visualized by atomic force microscopy, J. Mol. Biol. 285 (1999) 1347–1351.
[32] E.M. Nestorovich, T.K. Rostovtseva, S.M. Bezrukov, Residue ionization and ion transport through OmpF channels, Biophys. J. 85 (2003) 1–12.
[33] S.M. Bezrukov, J. Kasianowicz, Current noise reveals protonation kinetics and number of ionizable sites in an open protein ion channel, Phys. Rev. Lett. 70 (1993) 2352–2355.

[34] B. Prod'hom, D. Pietrobon, P. Hess, Direct measurement of proton transfer rates to a group controlling the dihydropyridine-sensitive Ca2+ channel, Nature 329 (1987) 243–246.
[35] C. Danelon, J. Grandl, R. Hovius, H. Vogel, Modulation of proton-induced current fluctuations in the human nicotinic acetylcholine receptor channel, Biochim. Biophys. Acta-Biomembranes 1768 (1) (2006) 76–89.
[36] R. Chiriac, T. Luchian, pH modulation of transport properties of alamethicin oligomers inserted in zwitterionic-based artificial lipid membranes, Biophys. Chem. 130 (2007) 139–147.
[37] C. Bachmeyer, F. Orlik, H. Barth, K. Aktories, R. Benz, Mechanism of C2-toxin inhibition by fluphenazine and related compounds: investigation of their binding kinetics to the C2II-channel using the current noise analysis, J. Mol. Biol. 333 (2003) 527–540.
[38] A.S. Verkman, A.K. Solomon, Kinetics of phloretin binding to phosphatidylcholine vesicle membranes, J. Gen. Physiol. 15 (1980) 673–692.
[39] J. Reyes, F. Greco, R. Motais, R. Latorre, Phloretin and phloretin analogs: mode of action in planar lipid bilayers and monolayers, J. Membr. Biol. 72 (1983) 93–103.
[40] P. Pohl, T.I. Rokitskaya, E.E. Pohl, S.M. Saparov, Permeation of phloretin across bilayer lipid membranes monitored by dipole potential and microelectrode measurements, Biochim. Biophys. Acta 1323 (1997) 163–172.
[41] A.S. Verkman, A.K. Solomon, Kinetics of phloretin binding to phosphatidylcholine vesicle membranes, J. Gen. Physiol. 75 (1980) 673–692.
[42] F. Schmidtchen, M. Berger, Artificial organic host molecules for anions, Chem. Rev. 97 (1997) 1609–1646.
[43] R. Dutzler, G. Rummel, S. Alberti, S. Hernandez-Alles, P. Phale, J. Rosenbusch, V. Benedi, T. Schirmer, Crystal structure and functional characterization of OmpK36, the osmoporin of *Klebsiella pneumoniae*, Structure 7 (1999) 425–434.
[44] B. Schmid, L. Maveyraud, M. Kromer, G.E. Schulz, Porin mutants with new channel properties, Protein Sci. 7 (1998) 1603–1611.
[45] R.L. Duffin, M.P. Garrett, K.B. Flake, J.D. Durrant, D.D. Busath, Modulation of lipid bilayer interfacial dipole potential by phloretin, RH421, and 6-Ketocholestanol as probed by gramicidin channel conductance, Langmuir 19 (2003) 1439–1442.
[46] C. Grosman, A. Auerbach, Asymmetric and independent contribution of the second transmembrane segment 12′ residues to diliganded gating of acetylcholine receptor channels: a single-channel study with choline as the agonist, J. Gen. Physiol. 115 (2000) 637–651.
[47] S. Varma, E. Jakobsson, Ionization states of residues in OmpF and mutants: effects of dielectric constant and interactions between residues, Biophys. J. 86 (2004) 690–704.
[48] S. Varma, S.W. Chiu, E. Jakobsson, The influence of amino acid protonation states on molecular dynamics simulations of the bacterial porin OmpF, Biophys. J. 90 (2006) 112–123.